DEVELOPMENT OF A GAS TURBINE GENERATOR WITH A 20 MM ROTOR

J. Peirs[1], R. Van Den Braembussche[2], P. Hendrick[4], M. Baelmans[1], J. Driesen[1], R. Puers[1], F. Al-Bender[1], T. Waumans[1], P. Vleugels[1], E. Ferraris[1], K. Liu[1], Z. Alsalihi[2], A. Di Sante[2], T. Verstraete[2], J. Grossen[3], P. Bécret[3], J. Trilla[3], T. Stevens[1], F. Rogiers[1], S. Stevens[1], F. Ceyssens[1], D. Reynaerts[1]

[1]Katholieke Universiteit Leuven, Belgium
[2]von Karman Institute for Fluid Dynamics, Belgium
[3]Royal Military Academy, Belgium
[4]Université Libre de Bruxelles, Belgium

Abstract: This paper reviews the status of the Belgian PowerMEMS project [1]. Focus is on the technology developments for realizing a 20 mm diameter hydrogen-based gas turbine. The total device consists of a compressor, turbine, combustion chamber, generator and recuperator. It has a total diameter of 100 mm and is 112 mm long, and has an expected electrical power output in the order of 1 kW.

Key Words: Micro gas turbine, microgenerator

1. INTRODUCTION

In the last decade, several institutes have been developing miniaturised turbines [2-4]. Two distinct approaches to this engineering problem have been proposed: a layer-by-layer MEMS-based approach [2] mostly resulting in ultimate miniaturization and an approach based on the miniaturization of "conventional" manufacturing [3,4]. In our case we also opted for a "conventional" approach resulting in a targeted rotor diameter of 20 mm running at 500,000 rpm.

2. GENERAL LAYOUT

Figure 1 shows the general layout of the microturbine generator. The system basically consists of a compressor, recuperator, combustion chamber, turbine and electrical generator. In total it has a diameter of around 100 mm and a length of 110 mm. The compressor and turbine impellers are 20 mm in diameter. In order to accomodate the relatively large volume of both the combustion chamber and the recuperator in a compact way, an annular design was chosen for both components.

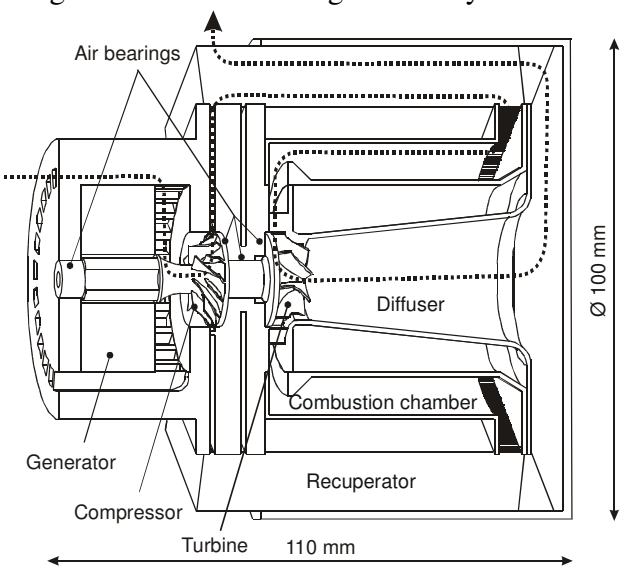

Fig. 1: Gas turbine generator layout.

As a consequence of the adopted layout, the hottest part - the combustion chamber - is enclosed by the recuperator on the outside and by the exhaust diffuser on the inside. This allows to recycle heat losses from the combustion chamber.

To avoid demagnetisation of the magnets, the generator is located away from the hot parts and the inlet air is aspirated through cooling channels in the generator stator.

An exhaust diffuser is added to create a sub-ambient pressure at the turbine exit, such that more power can be extracted.

Generator, compressor and turbine are mounted on a single shaft for simplicity and reliability.

3. THERMODYNAMIC CYCLE

The thermodynamic cycle has been determined and optimised in an iterative way. Fixed values are the compressor diameter (20 mm), nominal shaft speed and max. turbine inlet temperature (TIT). The max. TIT is set by material limits to 1200 K. The nominal shaft speed was set to 500,000 rpm as models predicted that with the

given compressor diameter, a pressure ratio of 3 is achievable. Below this value efficiency drops sharply, while higher values offer smaller efficiency improvements.

A detailed gas turbine model was built containing compressor and turbine maps, and models for the combustion chamber and recuperator. An iterative process was used to optimise the efficiency of the individual components as well as the global cycle. The following parameters were obtained:

- Nominal mass flow: 20 g/s
- Pressure ratio: 3.0
- Power
  - Compressor: 3800 W
  - Turbine: 5083 W
  - Net mechanical output: 1180 W
- t-s polytropic efficiency
  - Compressor: 66 %
  - Turbine: 78 %
- Turbine inlet temperature: 1200 K
- Cycle efficiency
  - Without recuperation: 11 %
  - With recuperation: 20 %

While the primary goal of the optimisation was the maximisation of the cycle efficiency, a major result was an enlargement of mass flow and power, this way reducing thermal and flow losses in a relative sense.

An off-design analysis has been performed to investigate stability, transient behaviour and start-up. Figure 2 shows the mechanical power as a function of speed and TIT, indicating that a minimal TIT of 600 K is required for start-up.

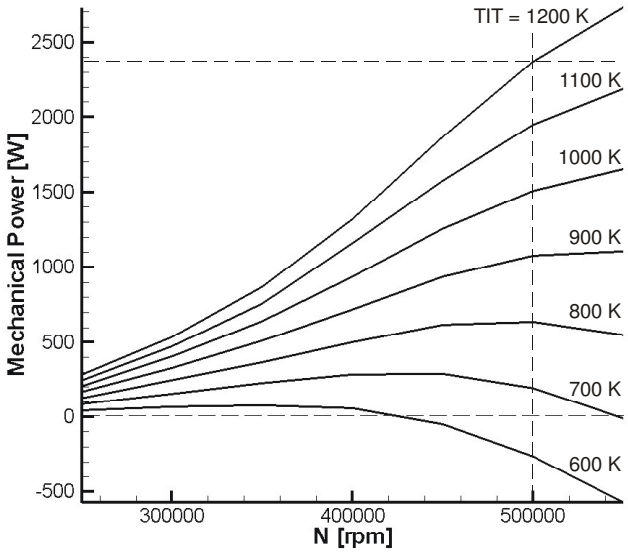

Fig. 2: Mechanical power vs. speed and turbine inlet temperature (TIT) (without recuperator).

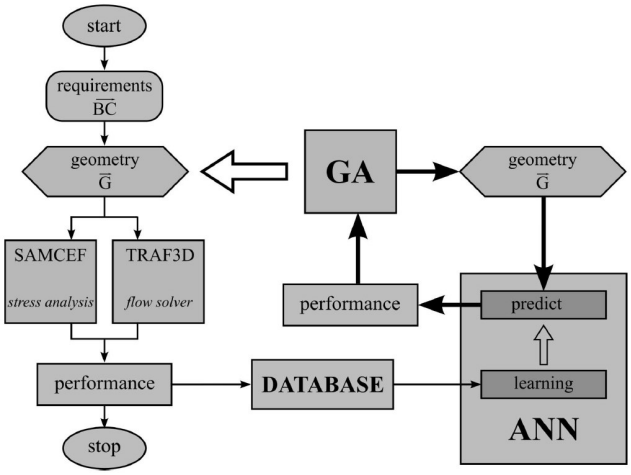

Fig. 3. Flow chart of the optimization algorithm .

4. IMPELLER OPTIMISATION

A new multidisciplinary design method [5] is used to find a compromise between the conflicting demands of high efficiency and low centrifugal stresses in the blades. Simultaneous analyses of the aero performance and stress predictions replace the traditional time consuming iterative design approach.

The system (Fig. 3) makes use of a Genetic Algorithm (GA), an Artificial Neural Network (ANN), a database, a Navier-Stokes solver (NS) and a Finite Element stress Analysis tool (FEA). The basic idea of this method is a two-level optimization. A first one uses a rapid but less accurate analysis method (ANN) to evaluate the large number of geometries generated by the GA. The optimum geometry, according to the ANN predictions, is then analyzed by the more accurate but much more computationally expensive Navier-Stokes and FEA stress calculations to verify the accuracy of the ANN predictions. The outcome of such an optimization cycle is added to the database. After a new training on the extended database, the ANN will be more accurate as it is based on more information and the outcome of the next GA optimization will be closer to the real one. The optimization cycle is repeated until the Navier-Stokes and FEA results confirm the accuracy of the ANN predictions.

The resulting impeller geometries and corresponding centrifugal stresses are shown in

figure 4. Notice the large inlet diameter of the compressor (6 mm), being a compromise between shaft stiffness and aerodynamic performance.

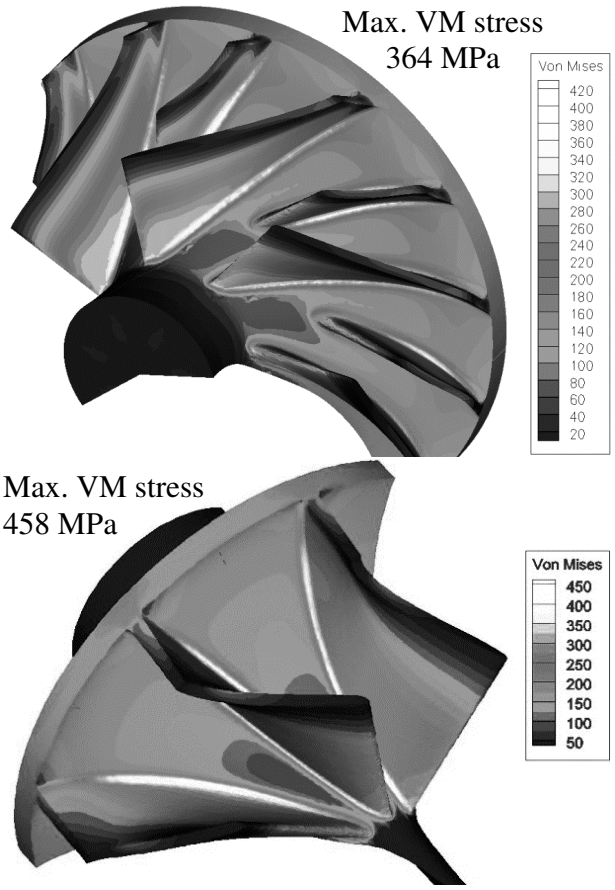

Fig. 4. Von Mises stresses in the optimised compressor (top) and turbine (bottom) geometries.

5. HIGH-SPEED BEARINGS

The system is relying on air bearings designed for optimal performance and stability at high running speeds. Two alternatives are investigated: aerodynamic foil bearings [6] and aerostatic bearings [7]. Aerostatic bearings are used for initial test set-ups, while the final device will preferentially use aerodynamic foil bearings, yielding a more autonomous system. Speeds up to 508,000 rpm have been demonstrated for a simplified rotor on aerostatic bearings.

6. GENERATOR

For reasons of mechanical strength (centrifugal load), a switched reluctance machine is chosen for the generator. The generator's rotor and magnetic

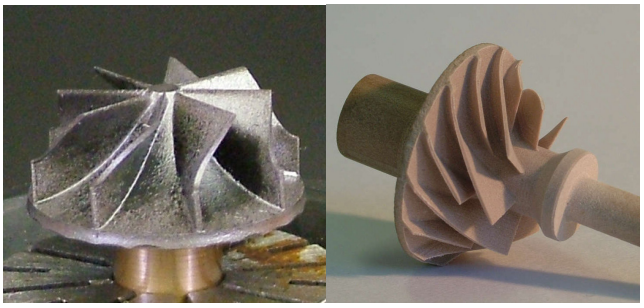

Fig. 5: Impeller prototypes. Left: ceramic turbine. Right: compressor. Both diameter 20 mm.

core have a laminated structure to minimize eddy current losses. A novel nanocrystalline material is used to reduce the losses at high-frequency operation. After heat treatment, the foil-shaped material is laminated into a stack using epoxy glue and subsequently machined.

7. PRODUCTION

The rotor and bearing geometries are the most critical components for production. Bearing surfaces have to be produced and aligned with micrometer accuracy. Especially the bearing surfaces on the rotor are critical as this rotor consists of 4 assembled components.

Compressor and turbine impellers have a complex 3D blade geometry due to their axial-radial design. Unigraphics NX 3.0 CAD/CAM software is used for modelling and tool path generation.

The titanium (Ti-6Al-4V) compressor is produced by 5-axis milling on a Kern micromilling machine, with tools down to 0.5 mm in diameter. The blank including the precise bearing and mating surfaces is machined on a Hembrug lathe.

The ceramic turbine is produced by die-sinking electrical discharge machining (EDM) [8]. An electrically conductive ceramic composite is chosen with good mechanical, thermal and machining properties: Si_3N_4-TiN. The graphite EDM electrodes are machined by 3-axis micromilling. The roughness after EDM is 2.3 µm Ra, such that postprocessing by grinding or abrasive flow machining is required

The ceramic bearing surfaces on the turbine´s backside are finished with diamond grinding tools to micrometer tolerances and 0.10 µm Ra.

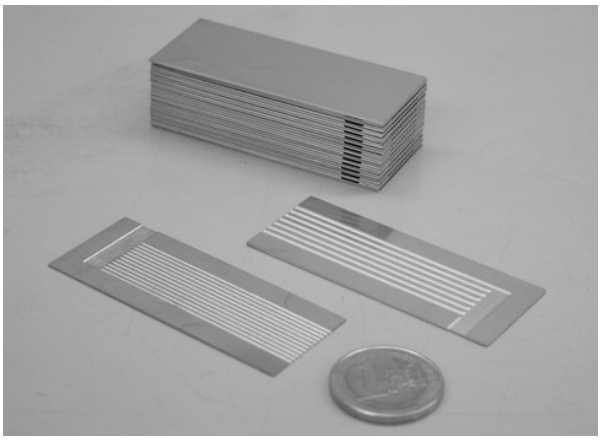

Fig. 6: Stacked recuperator block and individual hot and cold plates.

9. RECUPERATOR

The recuperator consists of 6 identical blocks positioned around the gas turbine. The design is determined by a multi-dimensional optimization in which cold and hot side recuperator pressure drops are used as optimization parameters [9]. The optimal design has a heat exchanger effectiveness of 74.5 % for relative pressure drops at cold and hot side of 8.5 kPa and 5.5 kPa respectively. The recuperator blocks consist of alternating hot and cold plates (52 in total), with longitudinal channels in counterflow (see fig. 6). Channels and collectors are etched with a uniform depth in stainless steel plates, 63 by 25 mm in size. Total stack height is 34 mm.

10. CONCLUSION AND FUTURE WORK

Prototypes of key components have been produced. The next step is a proof of concept using a turboshaft set-up. This set-up consists of a shortened shaft with only the compressor and turbine mounted on air bearings. The turbine is driven with hot or cold compressed air and drives the compressor. This allows to measure both compressor and turbine maps, as well as to test the rotordynamic behaviour.

ACKNOWLEDGEMENT

This research is sponsored by the Institute for the Promotion of Innovation by Science and Technology in Flanders, Belgium and coordinated within the framework of EC NoE "Multi-Material Micro Manufacture". T. Waumans acknowledges the Fund for Scientific research Flanders.

REFERENCES

[1] *http://www.powermems.be*

[2] A. H. Epstein, Millimeter-scale, Micro-Electro-Mechanical Systems Gas Turbine Engines. *ASME Journal of Engineering for Gas Turbines and Power*, vol. 126, pp. 205-226, 2004.

[3] S. Kang, J. P. Johnston, T. Arima, *et al.* Micro-scale radial-flow compressor impeller made of silicon nitride: manufacturing and performance, *Proc. ASME Turbo Expo*, Atlanta, USA, 2003, GT2003-38933.

[4] K. Isomura, M. Murayama, S. Teramoto, *et al.* Experimental verification of the feasibility of a 100W class micro-scale gas turbine at impeller diameter 10mm. *PowerMEMS Workshop*, Tokyo, Japan, 2005, pp. 25-28.

[5] T. Verstraete, Z. Alsalihi, R.A. Van den Braembussche, Multidisciplinary optimization of a radial compressor for micro gas turbine applications, *Proc. GT2007 ASME Turbo Expo 2007*, Montreal, Canada, 2007, GT2007-27484, 9 pages.

[6] P. Vleugels, T. Waumans, J. Peirs, F. Al-Bender, D. Reynaerts, High-speed bearings for micro gas turbines: stability analysis of foil bearings, *J. Micromech. Microeng.*, Vol. 16, No 9, pp. 282-289, 2006.

[7] T. Waumans, P. Vleugels, J. Peirs, F. Al-Bender, D. Reynaerts, Rotordynamic behaviour of a micro-turbine rotor on air bearings: modelling techniques and experimental verification, *Proc. Int. Conf. on Noise and Vibration Engineering (ISMA)*, Leuven, Belgium, 2006, pp. 181-197.

[8] K. Liu, E. Ferraris, J. Peirs, B. Lauwers, D. Reynaerts, Process Investigation of Precision Micro-Machining of Si3N4-TiN ceramic composite by Electrical Discharge Machining (EDM), *Proc. ISEM XV*, Pittsburgh, PV, USA, 2007, pp 221-226.

[9] T. Stevens, F. Rogiers, M. Baelmans, Integrated design of a micro recuperator in a gas turbine cycle, *PowerMEMS Workshop*, Freiburg, Germany, 2007, 4 pages.